

1 <https://doi.org/10.1016/j.seppur.2020.117828>

2 **Understanding the microbial trends in a nitrification reactor fed**  
3 **with primary settled municipal wastewater**

4 *Alba Pedrouso<sup>a\*</sup>, David Correa-Galeote<sup>b</sup>, Paula Maza-Márquez<sup>b,‡</sup>, Belén Juárez-Jimenez<sup>b</sup>, Jesús*  
5 *González-López<sup>b</sup>, Belén Rodelas<sup>b</sup>, Jose Luis Campos<sup>c</sup>, Anuska Mosquera-Corral<sup>a</sup> and Angeles Val*  
6 *del Rio<sup>a</sup>*

7 <sup>a</sup> CRETUS Institute, Department of Chemical Engineering, Universidade de Santiago de  
8 Compostela, E-15705, Santiago de Compostela, Spain. Email: alba.pedrouso@usc.es;  
9 anuska.mosquera@usc.es; mangeles.val@usc.es.

10 <sup>b</sup> Department of Microbiology and Institute of Water Research, University of Granada, 18071  
11 Granada, Spain. Email: dcorrea@ugr.es, paulamaza@ugr.es, belejj@ugr.es, jgl@ugr.es,  
12 mrodela@ugr.es

13 <sup>c</sup> Facultad de Ingeniería y Ciencias, Universidad Adolfo Ibáñez, Avda. Padre Hurtado 750,  
14 2503500, Viña del Mar, Chile. Email: jluis.campos@uai.cl.

15 <sup>‡</sup> present address: Microbial Ecology/Biogeochemistry Research Laboratory, NASA Ames  
16 Research Centre, CA, USA.

17

18 \* Corresponding author

19

20

21

22

23

24 **Abstract**

25 Partial nitritation was pointed out as the key step to implement the autotrophic nitrogen  
26 removal processes at low temperature. This study investigated the initiation and maintenance  
27 of a nitritation process with simultaneous COD removal in a sequencing batch reactor (SBR)  
28 run at 15 °C and fed with primary settled urban wastewater characterized by  $42 \pm 10$  mg  
29 DOC/L and  $45 \pm 4$  mg  $\text{NH}_4^+$ -N/L. A nitrite accumulation ratio of nearly 100 % was observed and  
30 the long-term (354 days) process stability was successfully maintained despite the municipal  
31 wastewater composition fluctuations. The absence of nitrite oxidizing bacteria (NOB) activity  
32 was attributed to the free nitrous acid (FNA) *in-situ* accumulated at high levels (0.02 – 0.20 mg  
33  $\text{HNO}_{2\text{A}}$ -N/L). Despite nitrate production was not observed, the quantification of bacterial  
34 groups indicated that NOB were present in the SBR sludge throughout the entire operational  
35 period. Ammonium oxidizing bacteria (AOB) abundance and community structure were  
36 significantly influenced by the organic matter present in the feeding. Average organic matter  
37 removal efficiencies of 80 % were obtained without observing any detrimental effect over the  
38 nitritation process performance, due to the functional redundancy within both the  
39 chemoheterotrophic and AOB communities.

40 **Keywords:** autotrophic nitrogen removal; free nitrous acid; low temperature; mainstream;  
41 nitrite oxidation inhibition.

## 42 **1. Introduction**

43 The combination of the partial nitrification (PN) and anammox (AMX) processes is one of the  
44 most promising alternatives for the fully autotrophic removal of nitrogen from wastewater [1,  
45 2]. Until now, PN/AMX technologies have been successfully implemented for the treatment of  
46 the reject waters of anaerobic sludge digesters in wastewater treatment plants (WWTPs),  
47 reducing the nitrogen load recirculated back to the mainstream. Driven by the outstanding  
48 economic and environmental associate benefits of the PN/AMX implementation, multiple  
49 efforts are focused on its application to the mainstream of WWTPs. When PN/AMX processes  
50 are applied for municipal wastewater treatment, the concentrations of COD which are  
51 commonly present (7 - 12 g COD/g N after primary settling) represent a shortcoming [2, 3].  
52 COD supports the development of aerobic heterotrophic bacteria, which compete with  
53 nitrifying bacteria for dissolved oxygen (DO), hindering the establishment of a steady-state  
54 autotrophic process. Moreover, nitrite oxidizing bacteria (NOB) activity suppression has been  
55 widely reported as one of the weakest points to achieve the nitrification process stability  
56 treating municipal wastewater (< 100 mg N/L) at low temperature (< 25 °C).

57 One of the most widely applied strategies to develop the nitrification process in a single unit  
58 relies on controlling the duration of the aerobic reaction phase based on the ammonia valley.  
59 In sequencing batch reactors (SBRs), as soon as ammonium oxidation was complete, an  
60 inflexion point (ammonia valley) in the pH profile was observed, since the oxidation of the  
61 nitrite to nitrate consumes less alkalinity [4]. The change from negative to positive in the value  
62 of  $dpH/dt$  was used to terminate the aeration. This strategy was successfully applied at low  
63 temperature, achieving a nitrite accumulation ratio (NAR) higher than 95 % [5] even at pilot-  
64 scale [4, 6]. However, if the alkalinity is limited to oxidize all the ammonium (i.e. nitrogen to  
65 inorganic carbon (N/IC) ratios higher than 0.6 g N/g IC) the pH will only decrease, and no  
66 ammonia valley will take place.

67 Among other strategies to implement the nitrification process under mainstream conditions, the  
68 feasibility of those based on the higher sensitivity of NOB to free nitrous acid (FNA)  
69 concentrations compared to ammonia oxidizing bacteria (AOB) stands out. NOB are  
70 completely inhibited at FNA concentrations of 0.023 mg HNO<sub>2</sub>-N/L, whereas 0.4 mg HNO<sub>2</sub>-N/L  
71 results in 50 % suppression of the AOB activity [7]. This approach was explored by exposing the  
72 sludge from the nitrification reactor to inhibitory FNA concentrations in an external unit [8-10],  
73 or producing it *in-situ* inside the nitrification reactor [11, 12]. As an advantage, the *in-situ*  
74 production of the FNA does not require pH adjustment nor sludge pumping to an external unit,  
75 reducing the sludge mechanical stress. Moreover, more extreme conditions are applied when  
76 the external unit is used that might also cause AOB activity reduction. However, these  
77 strategies based on the biocidal effect of FNA over NOB have been only tested treating mineral  
78 medium mimicking municipal wastewater [11, 12].

79 The success of the strategy proposed by Pedrouso, et al. [11] relies on the limitation of the  
80 N/IC ratio. This ratio must be theoretically higher than 0.6 g N/g IC in the wastewater fed to  
81 the nitrification reactor to maintain long-term process stability. The wastewater alkalinity  
82 depends mostly on the local source of freshwater. In this sense, it is necessary to corroborate  
83 if this strategy is adequate to be applied to municipal wastewater treatment.

84 Hence, the present study aims at demonstrating the feasibility of achieving and maintaining  
85 the long-term stability of a PN process by producing *in-situ* FNA in the presence of organic  
86 matter oxidation, in order to treat primary-settled municipal wastewater at low temperature  
87 (15 °C). The reactor performance and specific bacterial activities were monitored to evaluate  
88 the process stability. Furthermore, microbial community analyses were performed to  
89 understand how the changes of the operational parameters influenced bacterial community

90 structure and population dynamics as well as to corroborate if the operational strategy fosters  
91 AOB predominance over NOB.

## 92 **2. Materials and Methods**

### 93 **2.1. Reactor setup and operational conditions**

94 A 2-L nitritation reactor was operated as an SBR at  $15 \pm 1$  °C and the volume exchange ratio  
95 was fixed at 50 %. Air was supplied, and manually regulated, to the SBR through an air pump  
96 (KNF Labport) coupled to a coarse bubble diffuser to guarantee the complete mixture and  
97 oxygen supply for the biological reactions. Neither DO concentration nor pH value were  
98 controlled and ranged from 0.5 – 7.5 mg O<sub>2</sub>/L and 5.4 – 7.5, respectively (See Figure S1 in  
99 Supporting Material).

100 The operational period lasted 354 days divided into four Stages. In Stage I, synthetic medium  
101 was fed to the reactor containing 50 mg NH<sub>4</sub><sup>+</sup>-N [11]. Afterwards, primary settled municipal  
102 wastewater was fed during Stages II - IV (Table 1). At the end of Stage II, the sludge from the  
103 SBR was anoxically stored in the reactor medium at 4 °C for 25 days, and it was used in Stage III  
104 to restart the nitritation unit. Finally, in Stage IV, the applied organic matter and nitrogen loads  
105 decreased compared to previous stages, due to the decrease of those component  
106 concentrations in the used municipal wastewater as it was collected during rainy periods  
107 (winter time).

108 The SBR was operated using three different cycle distributions (See details in Figure S2,  
109 Supporting Material) controlled by a programmable logic controller (Siemens S7-224CPU).  
110 From day 0 to 142, the 3-hour cycle was distributed as 158 min of feeding and aeration, 20 min  
111 of settling and 2 min of withdrawal. On day 143, the cycle configuration was modified, and the  
112 aerated feeding lasted for 60 min, while 98 min were used just for aeration to decouple  
113 organic matter oxidation from the nitritation process. Finally, on day 334, the cycle length was

114 reduced from 180 min (8 cycles/day) to 144 min (10 cycles/day), shortening the hydraulic  
 115 retention time (HRT) from 6 h to 4.8 h.

116 **Table 1.** Feeding characteristics during the different operational stages.

Stage	Days	TN (mg N/L)	pH	IC (g IC/L)	NH <sub>4</sub> <sup>+</sup> -N/IC (g N/g IC)	TOC (mg/L)
S-I	0 – 137	50 ± 3	7.70 ± 0.10	55 ± 6	0.89 ± 0.02	-
S-II	138 – 182	33 ± 2	6.92 ± 0.09	41 ± 7	0.80 ± 0.05	40 ± 4
S-III	207 - 310	45 ± 10	7.20 ± 0.25	67 ± 8	0.68 ± 0.08	45 ± 9
S-IV	311- 354	20 ± 1	7.01 ± 0.09	26 ± 2	0.61 ± 0.02	22 ± 3

117 IC: Inorganic carbon; TN: total nitrogen; TOC: total organic carbon.

118

119 The SBR was seeded with 2.2 g VSS/L of suspended sludge from a PN/AMX reactor that treated  
 120 industrial saline wastewater (ca. 18 g NaCl/L) at 30 °C [13]. The measured maximum specific  
 121 activity (SA), at 15 °C, of AOB (SA<sub>AOB</sub>) was 11 ± 2 mg NH<sub>4</sub><sup>+</sup>-N/(g VSS·d), whereas NOB one (SA<sub>NOB</sub>)  
 122 was not detected.

## 123 2.2. Analytical methods

124 DO concentration and temperature in the bulk liquid were continuously measured (LDO  
 125 HQ40d, Hach Lange). Influent and effluent samples were periodically taken from the SBR. pH  
 126 values were determined with a Hach Sension<sup>+</sup> meter, and then, samples were filtered through  
 127 0.45 µm pore size filters before analysis. Spectrophotometric methods were used to determine  
 128 the ammonium [14], nitrite and nitrate [15] concentrations. Total organic and inorganic carbon  
 129 (TOC and IC) concentrations were measured with a Shimadzu analyzer (TOC-L CSN, Shimadzu).  
 130 Total nitrogen (TN) concentration was also measured in the TOC-L analyzer coupled with a  
 131 TNM-L Unit. The concentrations of total and volatile suspended solids (TSS and VSS) in samples

132 collected from the reactor and its effluent were determined according to Standard Methods  
133 [15]. Single operational cycles were also monitored in specific operational days to evaluate the  
134 evolution of the concentrations of the different compounds inside the reactor. Respirometric  
135 batch tests were periodically carried out to assess the SA following the methodology described  
136 by Lopez-Fiuza, et al. [16] and using a biological oxygen monitor (BOM, YSI Inc. model 5300).  
137  $SA_{AOB}$  and  $SA_{NOB}$ , as well as the aerobic heterotrophic activity ( $SA_{aerHET}$ ) when organic matter  
138 was fed to the SBR, were determined, in triplicates, at 15 °C. Equations for the FNA, NAR and  
139 ammonium oxidation ratio (AOR) calculations are included in Supporting Material.

### 140 **2.3. Quantification of microbial populations by quantitative PCR (qPCR)**

#### 141 **2.3.1. DNA extraction and purification of sludge samples for qPCR assays**

142 Samples were retrieved from the SBR after 138, 147, 153, 161, 166, 171, 231 and 266 days of  
143 operation (Stages II and III) for microbiological analyses. The samples were centrifuged (14,500  
144 × g, 1 min), and the sediments were frozen and kept at -20 °C. DNA was extracted from the  
145 sedimented samples and purified using the FastDNA-2 ml SPIN Kit for Soil and the FastPrep24  
146 apparatus (MP-BIO), following already described methods [17]. The quality and concentration  
147 of the DNA were measured with a NanoDrop ND-1000 Spectrophotometer (Thermo Scientific  
148 Waltham). DNA samples were stored at -20°C.

#### 149 **2.3.2. qPCR assays**

150 Total bacteria, ammonia oxidizing *Betaproteobacteria* (AOB), NOB (*Nitrospira* spp.) and AMX  
151 bacteria were quantified in the SBR samples by qPCR, using the molecular gene markers and  
152 primers summarized in Table S1A. Quantitative amplifications were performed in accordance  
153 with the MIQE guidelines [18], using True Start Hot Start DNA polymerase (Thermo Scientific)  
154 and SYBR Green I (Sigma Aldrich) in a total volume of 25 µl, with the aid of a QuantStudio-3  
155 Real-Time PCR system (Applied Biosystems). Previously described protocols were followed

156 [19]. The particular amplification conditions used for each reaction are summarized in Table  
157 S1B. For the absolute quantification of the target microbial groups, standard curves were  
158 constructed using a series of tenfold dilutions ( $10^{-1}$ - $10^{-8}$ ) of linearized plasmids carrying inserts  
159 of the target genes. Details on the plasmid standards used are provided in Supporting Material.  
160 All quantitative amplifications were performed in triplicates.

#### 161 **2.4. Illumina Miseq sequencing, DNA data processing and analysis**

162 Amplification of the V3-V4 region of the 16S rRNA gene was performed using the prokaryotic  
163 specific-primers Pro341F/Pro805R [20]. Raw data from Illumina sequencing process were  
164 analyzed using the Mothur MiSeq-pipeline and software mothur v1.43.0 [21]. The  
165 methodologies followed for alignment, OTU clustering and taxonomic classification are fully  
166 detailed in Supporting Material. The BLASTn suite (<http://blast.ncbi.nlm.nih.gov>) was used for  
167 manual sequence similarity analysis of AOB and NOB-related OTUs. Phylogenetic and  
168 molecular evolutionary analyses were conducted using MEGA version X [22]. A p-distance-  
169 based evolutionary tree was inferred from the partial 16S rDNA gene sequences using the  
170 Neighbor-Joining algorithm. A bootstrap test was conducted to infer the reliability of branch  
171 order, with a round of 1000 reassemblings. The OTUs sequences were deposited in the NCBI  
172 database under the accession number  
173 (<https://submit.ncbi.nlm.nih.gov/subs/genbank/SUB7677265>).

#### 174 **2.5. Statistical analysis**

175 The changes of the absolute abundances of the four targeted microbial groups throughout the  
176 sampling period were statistically analyzed using *IBM* SPSS Statistics v. 21 (SPSS Inc., USA) and  
177 R (R studio team, 2016; <http://www.r-project.org/>). The Kruskal-Wallis and Conover-Iman non-  
178 parametric tests ( $p < 0.05$  significance level) were used to search for differences among the  
179 groups of samples since the Shapiro-Wilk test indicated that the majority of the data sets did

180 not fit the normal distribution. The Primer software (PRIMER-E v. 6.0, Plymouth, UK) was used  
181 for the multivariate statistical analyses, following the protocols fully described elsewhere [17],  
182 and detailed in Supporting material.

### 183 **3. Results and discussion**

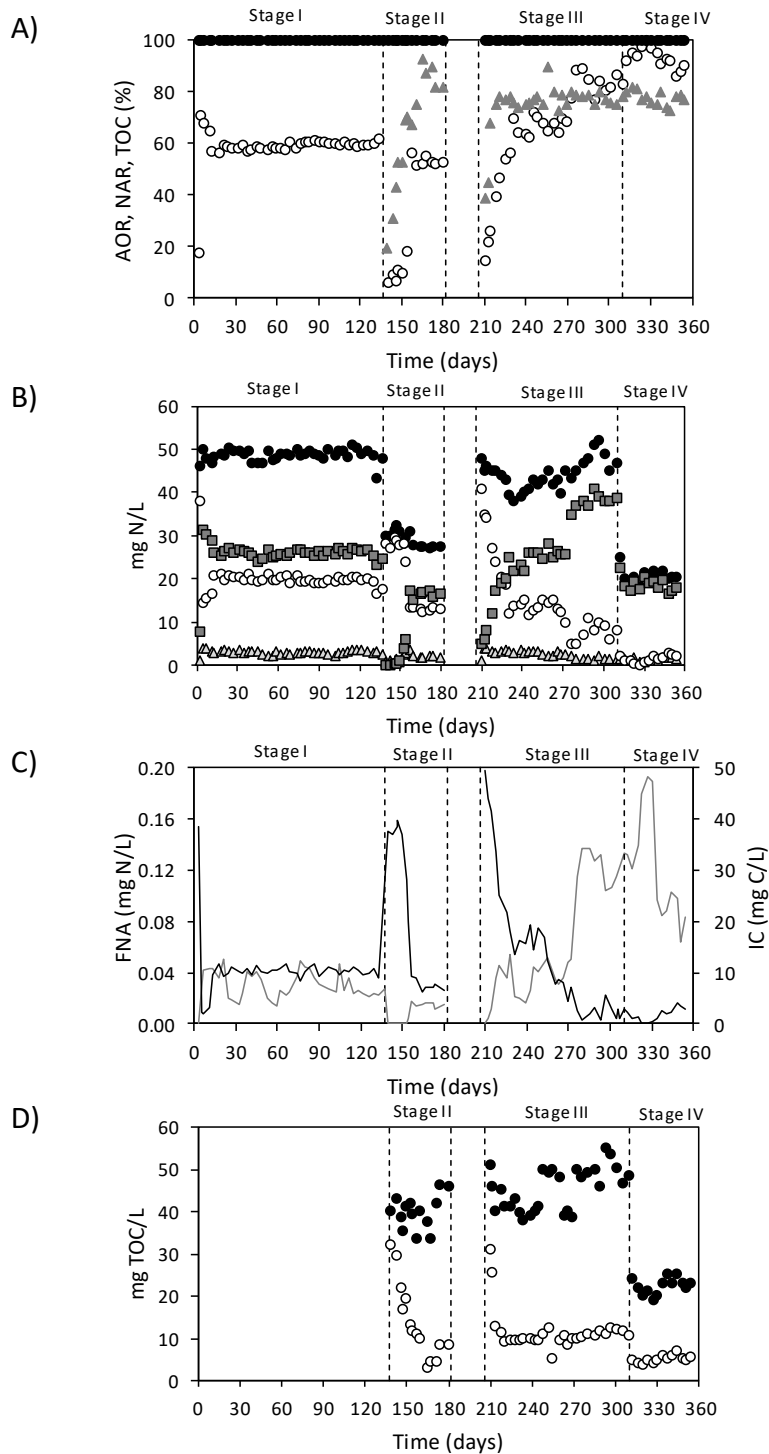
#### 184 **3.1. Nitrification establishment by natural *in-situ* FNA accumulation**

185 The SBR operated for 354 days fed with low ammonium concentrations ( $< 50 \text{ mg NH}_4^+\text{-N/L}$ )  
186 and at  $15 \text{ }^\circ\text{C}$  (Figure 1). In Stage I, despite the initial low  $SA_{\text{AOB}}$  of the inoculated biomass  
187 (Figure 2), the nitrification process was established fast. The AOR was already 20 % on day 3 and  
188 reached 60 % after 5 days of operation (Figure 1.A). Then, the nitrification process was  
189 successfully maintained with negligible nitrate production leading to a NAR of 100 % (Figure 1).  
190 Nitrate concentration in the effluent was already present in the influent. Despite IC in the  
191 effluent was not depleted ( $10 \pm 2 \text{ mg IC/L}$ , Figure 1.C) it was close to the alkalinity affinity  
192 constant value of  $6 \text{ mg IC/L}$ , commonly considered in the activated sludge modelling [23].  
193 Therefore, AOR could be either partially limited by the alkalinity concentration, by the DO  
194 concentration (Figure S1) and/or the cycle duration.

195 In this study, the nitrification process was successfully started-up using an inoculum with  
196 negligible  $SA_{\text{NOB}}$  without requiring any additional action. Although the inhibition caused on the  
197  $SA_{\text{NOB}}$  by salt concentrations above  $4 - 8 \text{ g NaCl/L}$  has been reported to be reversible [24, 25],  
198 NOB activity remained suppressed in the present nitrification reactor due to the *in-situ* FNA  
199 accumulation at concentrations ranging from  $0.02$  to  $0.08 \text{ mg HNO}_2\text{-N/L}$  (Figure 1.C).

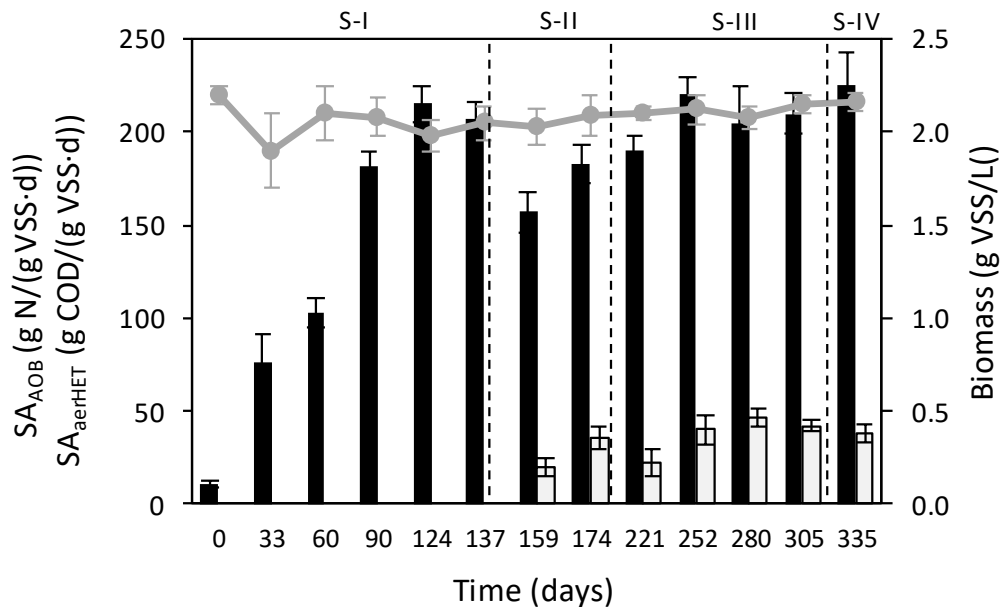
200 The progressive increase of the AOB activity during Stage I was confirmed by batch tests  
201 measuring  $SA_{\text{AOB}}$  up to  $207 \pm 9 \text{ mg NH}_4^+\text{-N}/(\text{g VSS}\cdot\text{d})$ , while  $SA_{\text{NOB}}$  was never detected (Figure 2).

202



203 Figure 1. Evolution of: A) Nitrite accumulation ratio (NAR, ●), ammonium oxidation ratio (AOR, ○) and  
 204 total organic carbon (TOC) oxidation ratio (▲), expressed in percentages; B) Concentrations of  $\text{NH}_4^+$  in  
 205 the influent (●) and  $\text{NH}_4^+$  (○),  $\text{NO}_2^-$  (■) and  $\text{NO}_3^-$  (△) in the effluent, expressed in mg N/L; C) Free nitrous  
 206 acid (FNA) concentration (—), in mg  $\text{HNO}_2\text{-N/L}$ , and inorganic carbon (IC) concentration (—), expressed as  
 207 mg IC/L; D) TOC concentration in the influent (●) and effluent (○) in mg TOC/L.

208 Pedrouso, et al. [11] already demonstrated the NOB suppression by *in-situ* FNA production  
 209 using a seeding sludge with relatively high  $SA_{NOB}$  and an initial NOB chemical inhibitor. These  
 210 authors hypothesized that when  $SA_{AOB}$  is higher than  $SA_{NOB}$ , it is possible to maintain the  
 211 nitrification process without chemicals addition as it was proven in the present study. In these  
 212 conditions, nitrite accumulates in the system, which leads to FNA inhibitory concentrations (if  
 213 the ratio of N/IC ranged from 0.6 to 1.0 g N/ g IC), simplifying the start-up of the nitrification  
 214 process.



215 Figure 2. Evolution of the maximum specific ammonium oxidizing bacteria activity ( $SA_{AOB}$ , ■) and specific  
 216 aerobic heterotrophic activity ( $SA_{aerHET}$ , □) in batch tests, and biomass concentration inside the  
 217 nitrification reactor (●) during the different Stages (S). Note that  $SA_{NOB}$  was also determined but it was  
 218 under the detection level of the measurement method during the whole operational period.  
 219

### 220 3.2. Performance of the nitrification and organic matter oxidation in the same unit

221 Primary settled municipal wastewater was fed to the SBR in Stage II (Table 1). This change in  
 222 the feeding provoked that, initially, the DO concentration raised from average values of 2.5 mg  
 223  $O_2/L$  to 6 mg  $O_2/L$  (Figure S1) as it was not consumed by AOB (no ammonium oxidation  
 224 occurred) either by heterotrophic bacteria due to their limited presence. On day 143, the SBR

225 operational cycle configuration was modified shortening the feeding phase to first promote  
226 the organic matter oxidation and once TOC concentration is low enable the ammonium  
227 oxidation (Figure S2). 15 days later, over 70 % of the incoming TOC was removed and  
228 approximately 50 % of the ammonium was oxidized to nitrite (Figure 1). The lower IC  
229 consumption led to higher pH values in the effluent compared to Stage I (Figure 1 and S1). The  
230 higher pH value and lower nitrite production caused the FNA concentration decrease close to  
231 the reported NOB inhibition values of 0.02 mg HNO<sub>2</sub>-N/L (Figure 1.C).

232 Despite the SBR operated for 44 days at FNA concentrations under the inhibitory values, NAR  
233 remained at 100 % (Figure 1.A) and SA<sub>NOB</sub> was not detected (Figure 2). These results confirm  
234 the robustness of the *in-situ* FNA strategy and are in good agreement with Pedrouso, et al. [11]  
235 that also observed a delay of more than 40 days to detect SA<sub>NOB</sub> when FNA concentrations fell  
236 below inhibitory values. Contrary, Duan, et al. [9] with an *ex-situ* FNA sludge treatment  
237 observed that NOB activity recovered as soon as the FNA treatment was stopped and despite  
238 the sludge treatment was restarted, the NAR recovery was limited to 30 %. One possible  
239 explanation is the fact that in the *ex-situ* treatment strategy, only a sludge fraction is exposed  
240 to the FNA in a limited period of time, while with the *in-situ* approach, sludge is continuously in  
241 contact with the FNA produced.

242 At the beginning of Stage II, when the organic matter started to be fed, the SA<sub>AOB</sub> decreased  
243 from 207 ± 9 to 157 ± 11 mg NH<sub>4</sub><sup>+</sup>-N/(g VSS·d) and later it was partially recovered (Figure 2). In  
244 the meanwhile, the SA<sub>aerHET</sub> reached values of 35 ± 6 mg COD/(g VSS·d) (Figure 2). Moreover,  
245 the biomass concentration inside the SBR remained at values of approximately 2 g VSS/L  
246 (Figure 2), while the effluent one slightly increased but it remained under 15 mg VSS/L (it was 6  
247 mg VSS/L in Stage I) resulting in solid retention times (SRT) decrease from 80 -100 days to 20 -  
248 30 days.

### 249 3.3. Recovery of oxidation processes after anoxic starvation

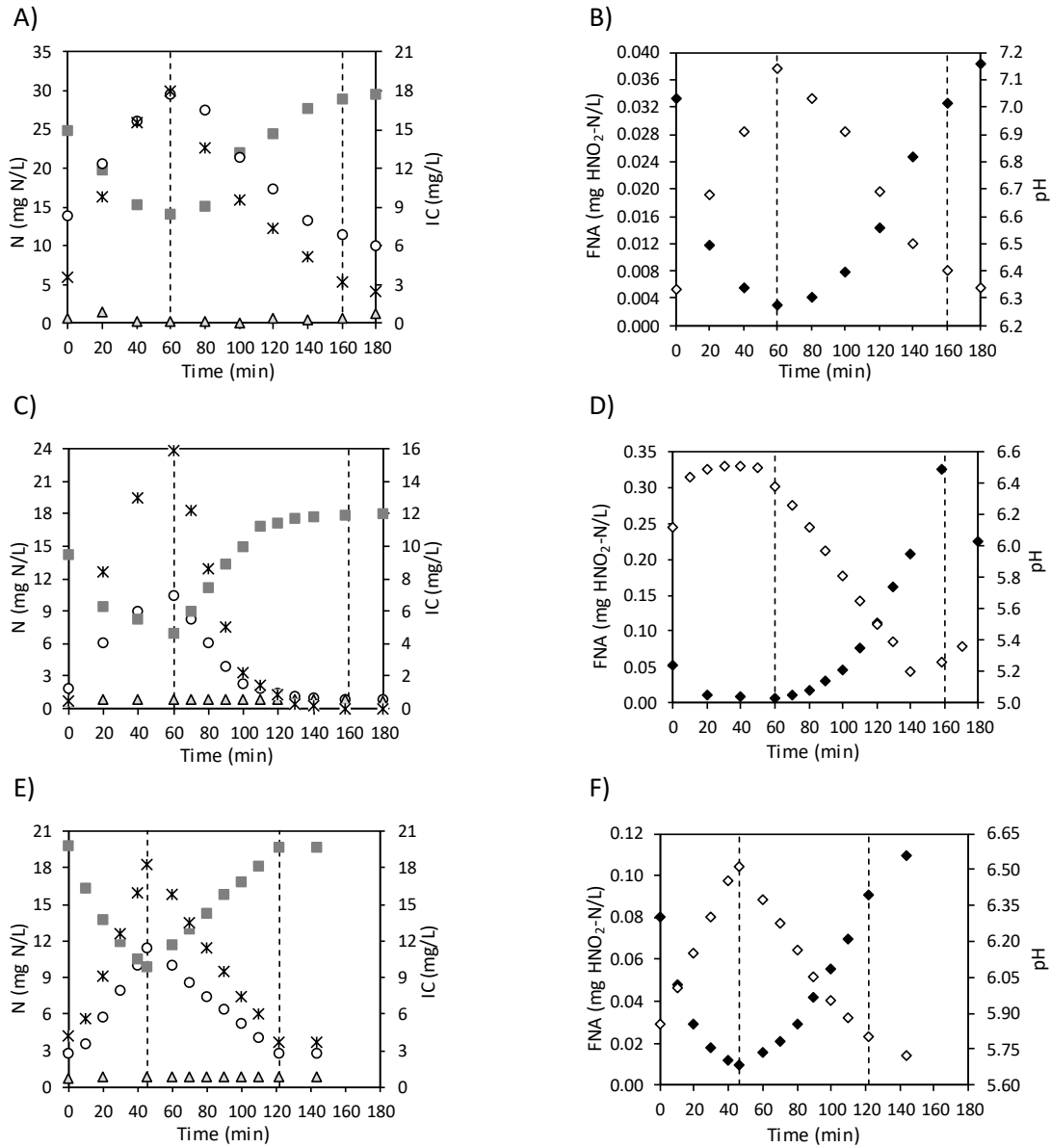
250 In Stage III, the SBR was restarted after 25 days stopped and it took approximately 12 days to  
251 recover the TOC oxidation of 70 % (Figure 1.A). Once TOC removal was re-established, the AOR  
252 rose exponentially and stabilized at 60 % after 6 days (day 225) without nitrate production  
253 (Figure 1.A and B). Nan, et al. [26] observed, from batch tests, that starvation periods (of 5  
254 days before or 12 hours after the FNA sludge treatment) enhanced the resistance of NOB to  
255 FNA. However, the starvation period before Stage III did not seem to affect the NOB  
256 suppression in the present study negatively.

257 The incoming N/IC ratio decreased from Stage II ( $0.80 \pm 0.05$  g N/g IC) to Stage III ( $0.68 \pm 0.08$  g  
258 N/g IC) (Table 1) and average pH values decreased to  $6.1 \pm 0.2$  (reaching minimum values of  
259 5.8, Figure S1). The lower pH value, combined with the higher nitrite concentration reached in  
260 the effluent (Figure 1.B), caused the increase of the FNA concentration to average values of  
261  $0.06 \pm 0.04$  mg  $\text{HNO}_2\text{-N/L}$  and up to  $0.13$  mg  $\text{HNO}_2\text{-N/L}$  (Figure 1.C), much higher than the NOB  
262 inhibitory threshold [7]. The high FNA values did not apparently affect the AOB activity and the  
263  $\text{SA}_{\text{AOB}}$  average values increased to  $210$  mg  $\text{NH}_4^+\text{-N}/(\text{g VSS}\cdot\text{d})$  (Figure 2).

264 During Stage III, the AOR further increased from the average  $67 \pm 7$  % (days 225 - 276) to  $85 \pm 3$   
265 %. On days 225 - 276, the AOR could be limited by the reaction fixed time and/or by the  
266 operational conditions imposed, such as the aeration flow rate. At the end of this Stage, the  
267 average N/IC ratio of  $0.68$  g N/g IC (Table 1) enables the oxidation of approximately 85 % (close  
268 to the obtained values). Therefore, the AOR was limited by the almost fully depleted IC  
269 concentration (Figure 1.C).

270 To deeply evaluate the nitrogen conversion in the reactor, on day 266 one SBR operational  
271 cycle was monitored (Figure 3.A and B). Once the feeding phase ended, pH, ammonium and IC  
272 concentrations dropped following a similar pattern. Consequently, nitrite concentration rose

273 from 14 to 30 mg  $\text{NO}_2^-$ -N/L leading to the *in-situ* FNA accumulation. The FNA concentrations  
 274 were higher than 0.02 mg  $\text{HNO}_2$ -N/L only in the last 40 min of the cycle (Figure 3.B). Even in  
 275 these conditions, nitrate production was not detected. The IC was almost entirely consumed  
 276 with 2 mg IC/L (Figure 3.A) at the end of the cycle.



277 **Figure 3.** SBR cycle characterization on day 266 (Stage III) (A, B) and on day 331 (C, D) and day  
 278 345 (E, F) (Stage IV). A, C, E) Evolution of ammonium (o), nitrite (■) and nitrate (Δ)  
 279 concentrations expressed as mg N/L and inorganic carbon (IC) concentration as mg IC/L (\*). B,  
 280 D, F) Evolution of the pH value (◇) and FNA concentration (◆) expressed as mg  $\text{HNO}_2$ -N/L.

### 281           **3.4. Optimization of the operational cycle to treat very low nitrogen concentrations**

282    In Stage IV, diluted wastewater was fed to the system characterized by a N/IC ratio was  $0.61 \pm$   
283     $0.02$  g N/g IC (Table 1), close to the stoichiometric ratio of  $0.59$  g N/g IC required for the  
284    complete oxidation of ammonium [11]. Thus, both ammonium and IC were almost entirely  
285    consumed (Figure 1). Due to the lack of enough alkalinity to buffer the system, pH values as  
286    low as  $5.3$  were obtained and in turn, the FNA concentration rose up to  $0.20$  mg  $\text{HNO}_2\text{-N/L}$ .

287    The cycle monitored on day 331 (Figure 3.C and D) proved that ammonium and IC were  
288    consumed before the end of the reaction period. As IC concentration decreased, the pH value  
289    sharply dropped. Thus, the FNA concentration augmented to values higher than  $0.30$  mg  
290     $\text{HNO}_2\text{-N/L}$  that might partially inhibit the AOB activity. According to Zhou, et al. [7],  $0.40$  mg  
291     $\text{HNO}_2\text{-N/L}$  resulted in a  $50\%$  suppression of the AOB activity, whereas Jiang, et al. [27]  
292    observed the  $57\%$  of the AOB activity was loss by exposing the sludge to FNA concentrations  
293    of  $1.2$  mg  $\text{HNO}_2\text{-N/L}$ . Although, as far as alkalinity is available, full ammonium abatement is not  
294    recommended and concentrations of  $2 - 5$  mg  $\text{NH}_4^+\text{-N/L}$  should remain to avoid limiting the  
295    AOB growth rate [28]. Contrary to the observed continuous reactors, in SBR systems, this  
296    effect should not be relevant since, from the major part of the cycle, higher ammonium  
297    concentrations were present (Figure 3.C).

298    To avoid part of the cycle that is inactive (ammonium is already oxidized), on day 334, the cycle  
299    length was shortened to  $144$  min (Figure S2). By doing this, the average pH values slightly  
300    increased (from  $5.56 \pm 0.10$  to  $5.79 \pm 0.06$ ; Figure S1) and the AOR decreased, obtaining  
301    ammonium concentrations around  $2 - 3$  mg  $\text{NH}_4^+\text{-N/L}$  in the effluent. This indicated that the  
302    reaction phase adjusted to the duration of the cycle (Figure 1 and 3) confirmed by the cycle  
303    characterization performed on day 345 that leads to a similar pattern to that observed in Stage  
304    III (Figure 3 E, F) with FNA concentration up to  $0.11$  mg  $\text{HNO}_2\text{-N/L}$ .

305 The average biomass concentration inside the reactor remained at 2 g VSS/L (Figure 2). The  
306  $SA_{AOB}$  was over 200 mg  $NH_4^+-N/(g\ VSS\cdot d)$  (Figure 2) which indicated that, despite the presence  
307 of organic matter, the ammonium oxidation capacity inside the reactor was 400 mg N/(L·d).  
308 Considering these results, the HRT might be further reduced, increasing the applied nitrogen  
309 load that was approximately  $150 \pm 42$  mg N/(L·d).

### 310 **3.5. Quantification of microbial groups by quantitative PCR (qPCR) and links to** 311 **operational parameters in the SBR**

312 The absolute abundances of gene markers of total Bacteria, AOB, NOB and AMX in samples  
313 retrieved from the SBR are displayed in Figure 4. The Kruskal-Wallis and Conover-Iman tests  
314 showed that there were significant differences among the samplings ( $p < 0.05$ ) for all the  
315 microbial groups quantified.

316 At day 138, when the SBR started being fed with primary settled municipal wastewater, the  
317 average abundance of gene markers of total Bacteria was  $1.33 \cdot 10^8 \pm 1.95 \cdot 10^7$  copies/100 ng  
318 DNA, which increased steadily for the next 15 days reaching  $5.31 \cdot 10^9 \pm 7.87 \cdot 10^8$  copies/100 ng  
319 DNA on day 153, and then remained without differences until the end of Stage II (Figure 4).  
320 Simultaneously, the average abundance of copies of the *amoA* gene abruptly decreased  
321 between days 138 and 147 (*ca.* 2 orders of magnitude), then recovered progressively up to day  
322 166, maintaining a similar abundance by the end of Stage II (day 171) (Figure 4).

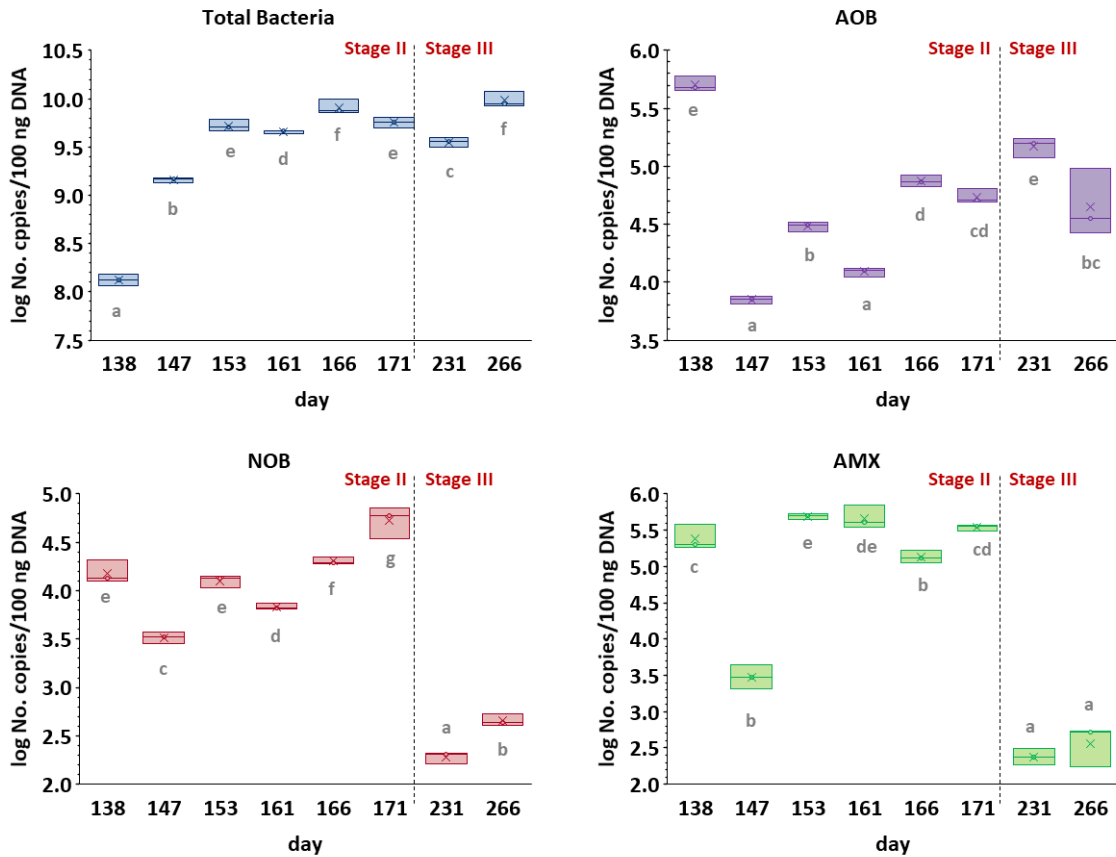
323 The shifts of the abundance of both total Bacteria and AOB were in accordance with the  
324 observed changes in the SBR system performance. Following the change of the feeding on day  
325 138, ammonia oxidation halted, leading to a severe reduction of the size of the AOB  
326 community, but the subsequent adjustment of the operational cycle configuration on day 143  
327 allowed for the successful adaptation of the community to achieve organic matter and  
328 ammonia oxidation in the same unit (section 3.2, Figure 1A). The observed patterns were

329 consistent with the previous knowledge on the response of nitrifiers to organic matter in  
330 WWTPs [29].

331 Regarding the samples analyzed during Stage III (days 231 and 266), the abundance of both  
332 Bacteria and AOB were similar or slightly higher than those measured at the end of Stage II  
333 (Figure 4), in agreement with the performance of organic carbon removal and AOR (76 - 79 %  
334 and 69 - 79 %, respectively, Figure 1A), and indicating the full recovery of both functional  
335 communities 20 days after the anoxic starvation step. AOB display a variety of physiological  
336 traits and molecular mechanisms advantageous for their survival under the limitation of  
337 ammonia or DO, which compensate for their lower growth rates compared to most  
338 chemoorganoheterotrophic bacteria [30], enabling them to regain activity in a short time after  
339 starvation periods. The abundance of gene markers of NOB was maintained in the range of  $10^3$   
340 -  $10^4$  copies/100 ng DNA throughout Stage II (Figure 4), but their activity was negligible in the  
341 SBR operation (Figure 1) and according to the respirometric assays (Figure 2). In contrast with  
342 the results observed for total Bacteria and AOB, the quantifications of NOB in the two samples  
343 of Stage III rendered values close to the limit of detection of the qPCR method. Several studies  
344 have previously reported that NOB are more sensitive than AOB to starvation and take longer  
345 to recover their metabolic activity after addition of substrates [31, 32]. The difference of the  
346 activity recovery rates among AOB and NOB has been related with a delayed transcriptional  
347 response of the *nxB* genes to the addition of substrates, which require longer periods than  
348 the *amoA* genes, leading to the subsequent dominance of AOB over NOB populations [33].

349 Nonetheless, nitrification gene markers were quantified in the SBR until day 266, 59 days after  
350 the restart of the system, which are nearly twofold the recovery periods reported previously  
351 for NOB [31]. In this sense, the FNA concentrations measured in this period, falling within the  
352 range reported to 100 % inhibit nitrite oxidation, could induce the wash-out of NOB in  
353 nitrification systems [7].

354 A



355

356 B

day	Total bacteria	AOB	NOB	AMX
138	$1.33 \cdot 10^8 \pm 1.95 \cdot 10^7$	$5.12 \cdot 10^5 \pm 8.30 \cdot 10^4$	$1.55 \cdot 10^4 \pm 4.45 \cdot 10^3$	$2.55 \cdot 10^5 \pm 1.09 \cdot 10^5$
147	$1.44 \cdot 10^9 \pm 8.92 \cdot 10^7$	$7.09 \cdot 10^3 \pm 5.36 \cdot 10^2$	$3.29 \cdot 10^3 \pm 4.39 \cdot 10^2$	$3.13 \cdot 10^3 \pm 1.16 \cdot 10^3$
153	$5.31 \cdot 10^9 \pm 7.87 \cdot 10^8$	$3.05 \cdot 10^4 \pm 2.85 \cdot 10^3$	$1.28 \cdot 10^4 \pm 1.86 \cdot 10^3$	$4.89 \cdot 10^5 \pm 3.98 \cdot 10^4$
161	$4.54 \cdot 10^9 \pm 1.81 \cdot 10^8$	$1.24 \cdot 10^4 \pm 1.10 \cdot 10^3$	$6.82 \cdot 10^3 \pm 5.55 \cdot 10^2$	$4.85 \cdot 10^5 \pm 1.84 \cdot 10^5$
166	$8.20 \cdot 10^9 \pm 1.46 \cdot 10^9$	$7.47 \cdot 10^4 \pm 9.10 \cdot 10^3$	$2.02 \cdot 10^4 \pm 1.61 \cdot 10^3$	$1.36 \cdot 10^5 \pm 2.83 \cdot 10^4$
171	$5.71 \cdot 10^9 \pm 7.43 \cdot 10^8$	$5.50 \cdot 10^4 \pm 8.40 \cdot 10^3$	$5.54 \cdot 10^4 \pm 1.92 \cdot 10^4$	$3.44 \cdot 10^5 \pm 3.41 \cdot 10^4$
231	$3.56 \cdot 10^9 \pm 4.12 \cdot 10^8$	$1.51 \cdot 10^5 \pm 2.90 \cdot 10^4$	$1.91 \cdot 10^2 \pm 2.67 \cdot 10^2$	$2.42 \cdot 10^2 \pm 6.30 \cdot 10^1$
266	$9.69 \cdot 10^9 \pm 1.90 \cdot 10^9$	$5.30 \cdot 10^4 \pm 3.83 \cdot 10^4$	$4.58 \cdot 10^2 \pm 6.72 \cdot 10^2$	$4.10 \cdot 10^2 \pm 2.05 \cdot 10^2$

357

358 **Figure 4. A.** Box-plots showing the logarithm of the number of copies/100 ng DNA of the

359 targeted genes markers of total Bacteria, AOB, NOB, and AMX, quantified by qPCR in the SBR.

360 **B.** Average  $\pm$  standard deviation of the number of copies of the targeted gene markers per 100

361 ng DNA in the SBR. The medians of boxes marked with the same letter in each plot are not

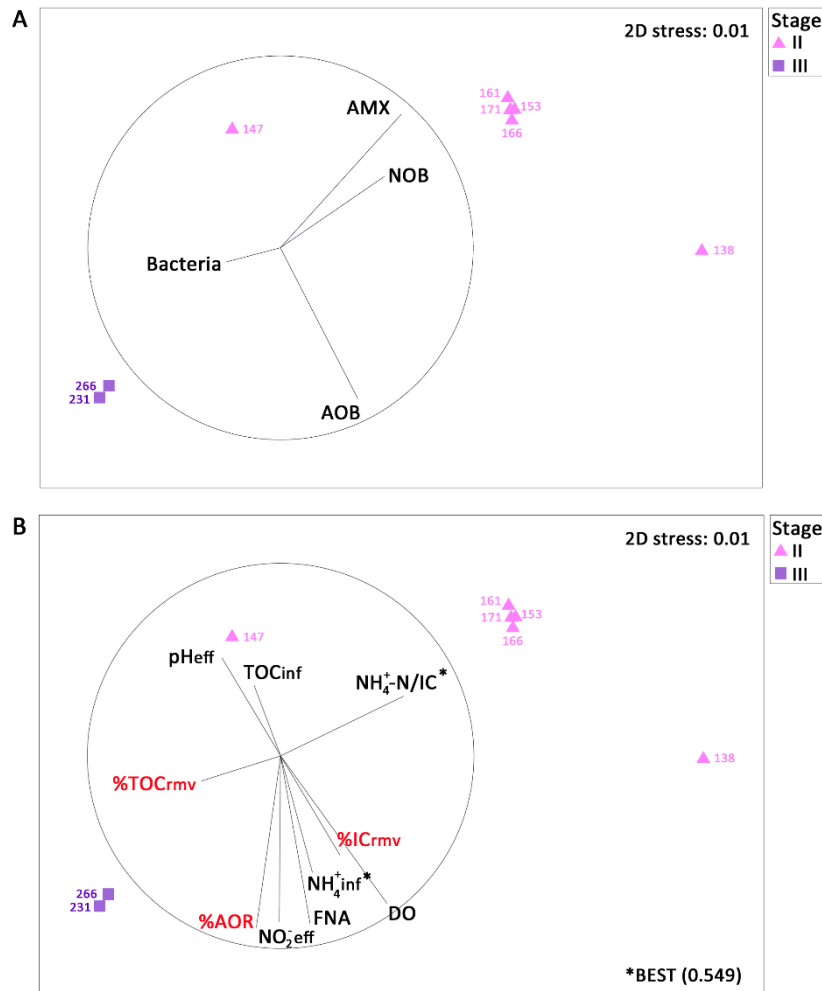
362 significantly different, according to the Conover-Iman test ( $p < 0.05$ ).

363 Except on day 177, the *amoA/nxrB* ratio (calculated from data shown in Figure 4B) was always  
364 > 1, indicating the dominance of AOB within the nitrifying community, and in agreement with  
365 the higher activity of AOB over NOB measured throughout both Stages II and III. These results  
366 indicated that the *in-situ* FNA strategy succeeded to effectively inhibit NOB in the SBR (Figure  
367 1) even when populations of this functional group were not wholly absent in the sludge. In this  
368 sense, an earlier study also reported the occurrence of NOB in short-cut biological N removal  
369 treatment systems, even when high nitrification rates (> 96 %) were being achieved [34].

370 Although the aim of this study was to develop only the nitrification process, AMX were present  
371 in the SBR sludge, as they were already present in the inoculum coming from a PN/AMX [13].  
372 The abundance of AMX gene markers followed similar patterns to that of AOB during Stage II  
373 (Figure 4), despite the operating conditions being unfavourable for AMX (Figure S1, Figure 1).  
374 Results are in agreement with those of previous studies detecting AMX in all compartments of  
375 full-scale municipal WWTPS. AMX often reach similar abundances than AOB, and can even  
376 grow under high COD/N ratios and DO concentrations >2 mg/L [35, 36]. Then, the AMX  
377 abundance in the SBR was drastically reduced in Stage III, indicating a poorer recovery capacity  
378 after anoxic starvation. Although AMX can survive through starvation periods, cell death is  
379 reported to account for >73 % of AMX decreased activity during anoxic starvation [37].

380 MDS and BIO-ENV statistical analyses were conducted in search of links among the shifts in the  
381 abundance of the four bacterial groups quantified by qPCR and the changes of the operational  
382 parameters and performance of the SBR (Figure 5, Table S2). AOB abundance displayed the  
383 strongest correlations with most of the abiotic variables included in the analysis (Figure 5,  
384 Table S2). In terms of SBR performance, strong positive correlations were observed with %  
385 AOR and % IC removal and the concentrations of NO<sub>2</sub><sup>-</sup> detected in the effluent ( $r > 0.800$ ). The  
386 number of copies of *amoA* genes were higher at increasing DO and NH<sub>4</sub><sup>+</sup> concentrations and at

387 lower amounts of TOC in the influent ( $r > 0.900$ ), all factors widely reported to benefit  
 388 nitrification [29]. In addition, AOB were the only bacterial group whose abundance was  
 389 significantly linked with increased acidity ( $r = 0.998$ ) and the generation of FNA ( $r = 0.956$ ).



390 **Figure 5.** Non-metric multidimensional scaling (MDS) ordination of the SBR samples from  
 391 Stages II and III, according to the abundance of copies of gene markers of total Bacteria, AOB,  
 392 NOB and AMX. Vectors on plots represent the trends of the abundance of each gene marker  
 393 (A) and the strength and directional influence of the operational parameters (B) throughout  
 394 the samples' ordination. %AOR, %TOC and %IC removal rates were also included in plot B to  
 395 illustrate the correlations among SBR performance and the abundances of the targeted  
 396 bacterial groups. The operation parameters which best explained the distributions of the  
 397 biological data according to BIO-ENV analysis are marked with an asterisk (\*).  
 398

399 The abundances of NOB and AMX displayed similar trends through the samples' ordination,  
400 and opposite to the behaviour observed for Bacteria (Figure 5A). According to BEST analysis,  
401 the concentration of  $\text{NH}_4^+$  in the influent and the  $\text{NH}_4^+\text{-N/IC}$  ratio contributed a major  
402 explanation (54.9 %) to the ordination of samples (Figure 5B, Table S2). Consistently with their  
403 metabolic features, both groups were strongly favored by higher  $\text{NH}_4^+\text{-N/IC}$  ratios ( $r > 0.900$ ),  
404 and displayed moderate negative correlations with the FNA concentrations ( $r = -0.415$  and  $r = -$   
405  $0.616$  for NOB and AMX, respectively) in agreement with the reported inhibitory activity of this  
406 compound to both groups of chemolithotrophs within the range of concentrations achieved in  
407 the SBR [7]. Contrary to the patterns observed for AOB, the correlation of the abundance of  
408 total Bacteria with the % TOC removal was robust and positive ( $r = 0.999$ ) (Figure 5, Table S2).

### 409 **3.6. Diversity of Bacteria in the SBR identified by Illumina sequencing and links to** 410 **operating parameters in the SBR**

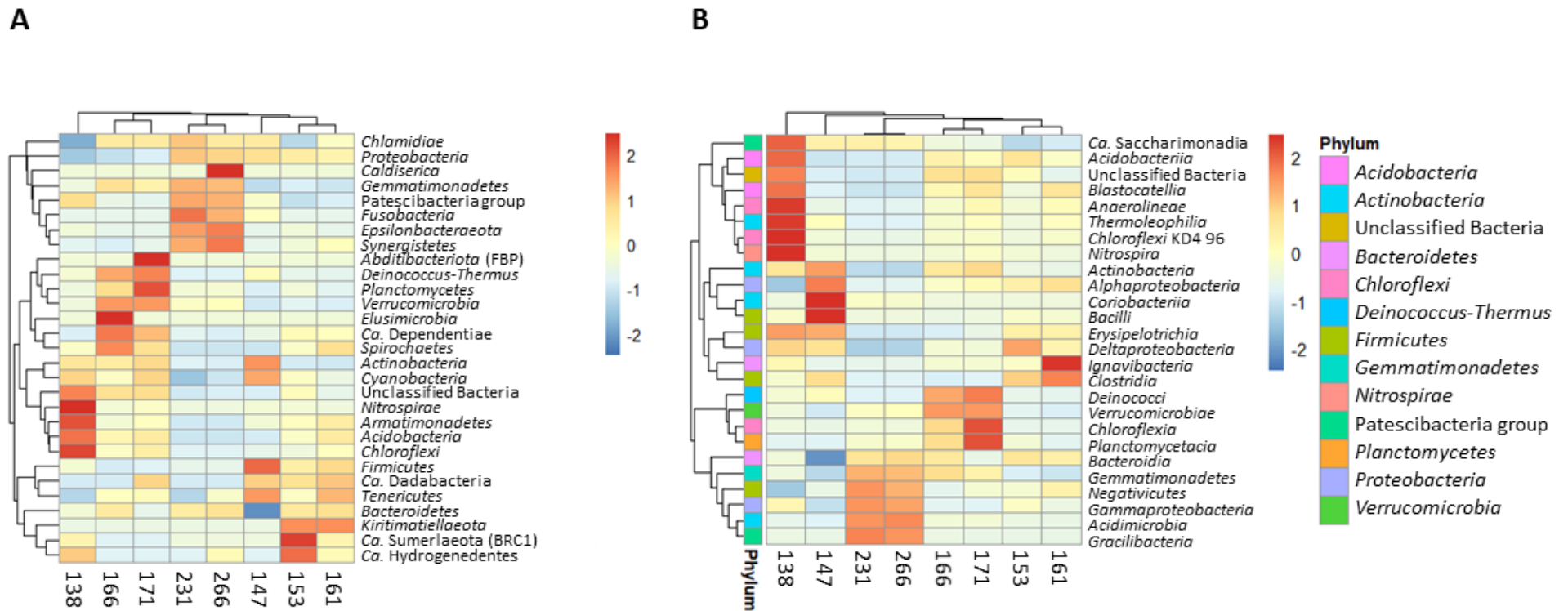
411 To complete the characterization of the bacterial community in the SBR, Illumina sequencing  
412 of partial 16S-rRNA genes was conducted on the same set of samples that qPCR. The average  
413 numbers of reads, Good's coverage, and diversity indices (richness,  $S$ ; Simpson,  $D$ ; and  
414 Shannon-Wiener,  $H'$ ) are summarized in Table S3. Overall, the indices described bacterial  
415 communities displaying high species diversity and low functional organization, although the  
416 samples of Stage III had significantly lower values of  $S$  and  $H'$  and higher values of  $D$ , compared  
417 to those of Stage II, showing that the community was less diverse and became more  
418 specialized after the anoxic starvation, comprising a narrower spectrum of numerically  
419 prevalent populations.

420 The relative abundances of Bacteria identified in the SBR samples at the Phylum and Class  
421 levels are displayed in Fig. S3 (complete data set available in Table S4). A total of 4288 OTUs  
422 were classified in 29 different Phyla, while 528 OTUs (4.6 % of sequence reads) could not be

423 assigned to any known Phyla (Figure S3A). Overall, the bacterial community was dominated by  
424 members of the *Proteobacteria* (relative abundance  $38.4 \pm 0.73 - 59.5 \pm 0.2 \%$ ), followed by  
425 *Bacteroidetes* ( $5.8 \pm 0.1 - 23.8 \pm 0.1 \%$ ), *Actinobacteria* ( $7.7 \pm 0.2 - 19.8 \pm 0.1 \%$ ), *Firmicutes* ( $2.1$   
426  $\pm 0.1 - 11.5 \pm 0.3 \%$ ), and *Chloroflexi* ( $0.35 \pm 0.0 - 7.2 \pm 0.0 \%$ ), in accordance with previous  
427 descriptions of the diversity at the Phylum level in aerobic WWTPs, either based on  
428 conventional or advanced technologies [38, 39]. Members of 74 Classes were identified, of  
429 which 25 displayed a relative abundance  $> 0.1 \%$  (Figure S3B). The prevalent Classes were  
430 *Gammaproteobacteria* ( $16.5 \pm 0.1 - 45.4 \pm 0.1 \%$ ), *Alphaproteobacteria* ( $6.4 \pm 0.2 - 39.3 \pm 0.2 \%$ ),  
431 *Actinobacteria* ( $2.8 \pm 0.0 - 18.5 \pm 0.2 \%$ ), *Bacteroidia* ( $5.7 \pm 0.1 - 23.2 \pm 0.4 \%$ ) and *Clostridia* ( $1.4$   
432  $\pm 0.0 - 6.0 \pm 0.0 \%$ ). Among the *Gammaproteobacteria*, most OTUs (429) fell within the Order  
433 *Betaproteobacteriales* ( $6.2 \pm 0.2 - 38.4 \pm 0.2 \%$ ).

434 Figure 6 shows the hierarchical clustering of the samples according to the relative abundances  
435 of taxa at both Phylum and Class levels. The sample taken on day 138, when municipal  
436 wastewater started to be fed to the SBR, clustered apart in both heatmaps, and was  
437 characterized for the over-representation of Phyla *Acidobacteria*, *Armatimonadetes*,  
438 *Chloroflexi*, and *Nitrospirae*, and Classes *Acidobacteriia*, *Anaerolineae*, *Blastocatellia*, *Ca.*  
439 *Saccharimonadia*, *Chloroflexi* KD4 96, *Erysipelotrichia*, *Nitrospira*, and *Thermoleophilia*. From  
440 day 138 onwards, population succession lead to significant changes of community structure,  
441 and by day 147, Classes *Actinobacteria*, *Alphaproteobacteria*, *Bacilli* and *Coriobacteriia*  
442 increased their representation, while *Chloroflexia*, *Deinococci*, *Planctomycetacia* and  
443 *Verrucomicrobiae* became more abundant by the end of Stage II (days 166 and 171).

444



445

446 **Figure 6.** Heat maps showing the relative abundances of Bacteria at phyla (**A**) and class (**B**) levels (when higher than 0.1 % in at least one sample)

447 derived from Illumina sequencing data of the SBR samples retrieved during Stages II and III. Hierarchical clustering is based on average linkage

448 (unweighted pair group method using arithmetic averages).

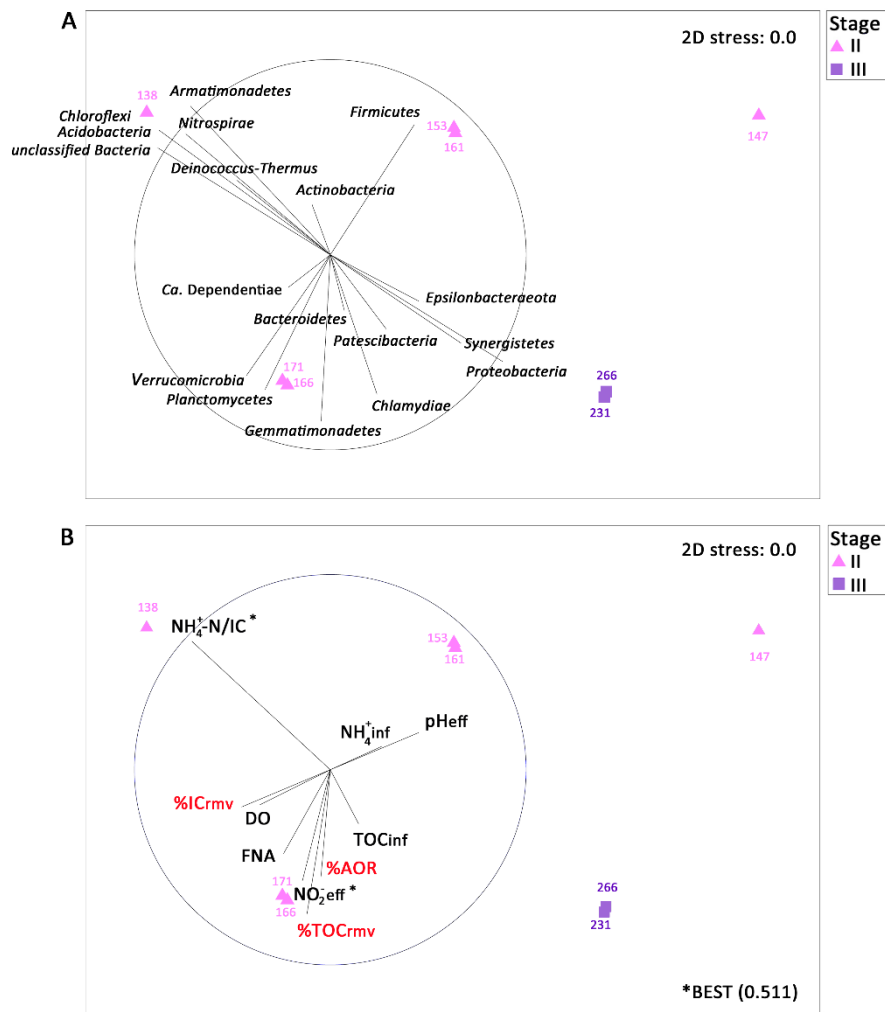
449 The samples taken during Stage III (days 231 and 266) were characterized by higher-than-  
450 average relative abundances of OTUs classified within the Phyla *Caldiserica*, *Chlamydiae*,  
451 *Epsilonproteobacteriaeota*, *Fusobacteria*, *Gemmatimonadetes*, Patescibacteria group,  
452 *Proteobacteria*, and *Synergistetes*, and Classes *Acidimicrobia*, *Bacteroidia*,  
453 *Gammaproteobacteria*, *Gemmatimonadetes*, *Gracilibacteria* and *Negativicutes*, indicating that  
454 the starvation stage favored the prevalence of these taxa once the SBR operation was  
455 restarted.

456 The shifts in the bacterial community structure taking place throughout Stages II and III were  
457 also reflected by the MDS ordination of the samples based on their community diversity  
458 (Figure 7). The BEST analysis indicated that the  $\text{NH}_4^+$ -N/IC ratio and the concentration of  $\text{NO}_2^-$  in  
459 the effluent provided the best explanation (51.1 %) to the observed changes of community  
460 patterns (Figure 7B). These variables significantly drove the shifts of *Nitrospirae* abundance,  
461 which were strongly favored by higher  $\text{NH}_4^+$ -N/IC ratios ( $r > 0.990$ ) and displayed moderate  
462 negative correlations with the concentration of  $\text{NO}_2^-$  in the effluent and %AOR (Table S5), in  
463 agreement with the results observed for qPCR data. Shu, et al. [40] previously described a  
464 positive relationship between the relative abundances of both AOB and NOB and higher  $\text{NH}_4^+$ -  
465 N/IC ratios, as well as negative correlations between the relative abundance of *Nitrospirae* and  
466 the  $\text{NO}_2^-$  concentration, in the effluent of a laboratory-scale simultaneous anammox and  
467 denitrification system.

468 Those Phyla which were over-represented in the initial sample of Stage II (*Acidobacteria*,  
469 *Armatimonadetes*, *Chloroflexi*, *Nitrospirae*) were favoured by the low input of organic matter  
470 to the SBR (Table S5). Conversely, 7 of the 18 Phyla displaying a relative abundance  $>0.1\%$  in at  
471 least one sample were strongly favored by higher TOC concentrations in the influent ( $r > 0.800$ ,  
472 Table S5). Among these, the numerically dominant groups *Proteobacteria* and *Bacteroidetes*  
473 comprise a majority of organoheterotrophic bacteria and are generally regarded as key players

474 for organic matter removal in biological wastewater processes based on different technologies  
475 [41, 42]. However, a strong correlation with TOC removal efficiency was only observed in the  
476 case of *Bacteroidetes* ( $r > 0.919$ , Table S5), indicating that members of these Phyla may play a  
477 particularly significant role under the conditions tested here. In this sense, *Bacteroidetes* are  
478 well known to specifically contribute to the hydrolysis and degradation of polymeric molecules  
479 in WWTPs [42].

480 Strong negative correlations were found among the concentrations of either  $\text{NO}_2^-$  or FNA and  
481 the relative abundances of *Firmicutes* ( $r < -0.90$ ) and *Actinobacteria* ( $r < -0.6$ ) (Fig. 7, Table S3).  
482 Nitrite is known for long as a potent inhibitor of species of *Firmicutes* [43], particularly those of  
483 the class *Clostridia* [44], which were the most abundant *Firmicutes* in the PN bioreactor (Figure  
484 S2). The biocidal effect of  $\text{NO}_2^-$  is thought to be related to the generation of FNA under acidic  
485 pH [44]. The effects of  $\text{NO}_2^-$  and its derived FNA on the community diversity of activated sludge  
486 were previously investigated in a PN/AMX system devoted to mainstream wastewater  
487 treatment [45] and a bioreactor for the acidic fermentation of waste sludge [46]. In both  
488 studies, the relative abundance of *Actinobacteria* decreased at higher FNA concentrations,  
489 while in the waste sludge fermentation system, FNA increased the overall relative abundance  
490 of *Firmicutes*, although it either favored or hampered that of particular *Clostridia* species.  
491 Accordingly, in a study conducted with pure cultures of ruminal bacteria it was found that  
492 *Butyrivibrio fibrisolvens* and *Ruminococcus flavefaciens* were sensitive to nitrite concentrations  
493 as low as 2 mg  $\text{NO}_2^-$ -N/L, while *R. albus* growth was unaffected [43]. The susceptibility to nitrite  
494 or FNA of microorganisms involved in wastewater treatment is acknowledged to vary widely,  
495 in agreement with the diversity of mechanisms through which this compound exerts its growth  
496 inhibitory and biocidal effects [44, 47].



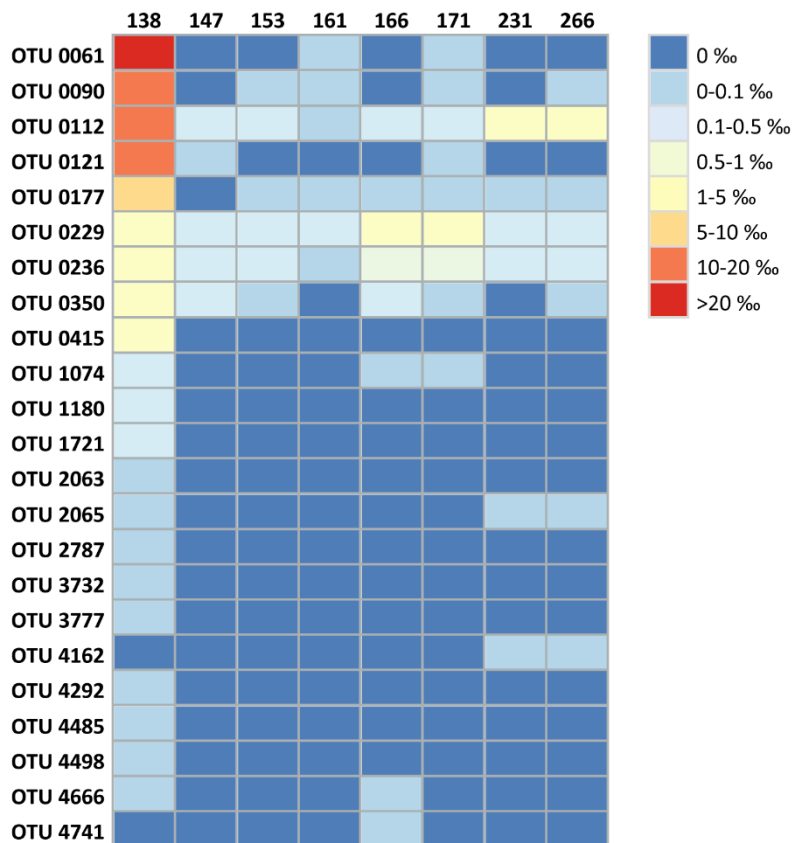
497

498 **Figure 7.** Non-metric multidimensional scaling (MDS) ordination of the SBR samples in Stages II  
 499 and III, according to the relative abundance of bacterial Phyla identified by Illumina  
 500 sequencing. Vectors on plots represent the trends of the relative abundance of each Phylum  
 501 (A) and the strength and directional influence of the operational parameters (B) throughout  
 502 the samples' ordination (only Phyla with relative abundance >0.1% in at least one sample are  
 503 shown). %AOR, %TOC and %IC removal rates were also included in plot B to illustrate the  
 504 correlations among SBR performance and the relative abundances of the different Phyla. The  
 505 operation parameters which best explained the distributions of the biological data according  
 506 to BIO-ENV analysis are marked with an asterisk (\*).

507 The subset of Illumina sequencing reads identified as phylogenetically close to known AOB and  
508 NOB genera were further analyzed to investigate the changes of the diversity of these  
509 functional groups occurring throughout Stages II and III (Figure 8). The relative abundance of  
510 AOB-related OTUs was 9.1 % on day 138, and ranged 0.04 - 0.26% in the rest of samples,  
511 following trends consistent with those observed for the absolute quantification of *amoA* gene  
512 copies. Twenty-three OTUs were classified as *Nitrosomonas*, while only one OTU (OTU 4839)  
513 occurring in low abundance and in a single sample (day 161) was closely related to  
514 *Nitrospira*. The AOB community was more diverse on day 138 (21 OTUs), compared to the  
515 rest of the samples (5-9 OTUs) (Figure 8).

516 The consensus sequences of 14 *Nitrosomonas*-related OTUs, which occurred in at least one  
517 sample with a frequency  $\geq 5$  sequence reads, were manually introduced in the BLASTn search  
518 tool of the NCBI nucleotide database and aligned to entries of 16S rRNA gene sequences of  
519 cultivated *Nitrosomonas* spp. strains, and a Neighbour-Joining tree was constructed to display  
520 their phylogeny (Figure S4). Eight OTUs (OTUs 0112, 0177, 0236, 0350, 1180, 1721, 2063 and  
521 2065) grouped with Cluster 6a strains (*N. oligotropha*-*N. ureae*), while 5 OTUs (OTUs 0061,  
522 0090, 0121, 0415 and 1074) fell within Cluster 7 (*N. europaea*-*N. eutropha*), and OTU 0229 lied  
523 between Clusters 6a and 6b, closest to 16S rRNA sequences of *N. marina* and *N. oligotropha*  
524 type strains (95.3 and 94.9% similarity, respectively). The OTUs dominating the community on  
525 day 138 (OTU 0061, OTU 0090 and OTU0121; 29, 18 and 14 ‰ relative abundances,  
526 respectively) belonged to Cluster 7 and were soon displaced after the change of feeding and  
527 cycling regime of the SBR by Cluster 6a-related OTUs, which kept dominating the AOB  
528 community after the anoxic starvation step (Figure 8, Figure S4). In Stage III, the AOB  
529 community became particularly specialized, being dominated by a single OTU (OTU 0112, 75.1  
530 - 81.7 % of sequence reads related to *Nitrosomonas* in days 231 and 266).

531 *Nitrosomonas* spp. of Clusters 7 and 6a frequently co-occur in laboratory- and full-scale  
532 nitrifying bioreactors (ie., [48, 49]), but their specific distribution patterns are highly influenced  
533 by the operational conditions [50]. Both cluster-level conserved features and strain-specific  
534 traits are determinant for niche differentiation and population succession [51]. Cluster 7  
535 members are regarded as r-strategists, having a low affinity for ammonia and prevailing in  
536 WWTPs with higher N loads, while Cluster 6a strains are considered K-strategists, displaying a  
537 higher affinity for their electron donor and being favored when ammonium concentrations  
538 become limiting for r-strategists [52]. In addition, genomes of Cluster 7 strains encode several  
539 proton pumping terminal oxidases with different affinities for DO, which provide a competitive  
540 advantage over Cluster 6a AOB under fluctuating DO concentrations [51], such as those  
541 provided when aeration was fully simultaneous to organic matter feeding in the SBR and AOB  
542 were forced to compete for DO with organoheterotrophs (days 138-143). The AOB community  
543 in the SBR was structured under autotrophic conditions during Stage I with an average  
544 concentration of NH<sub>4</sub>-N of ca. 50 mg/L (Figure 2B), and at the beginning of Stage II displayed a  
545 high species diversity but was dominated by Cluster 7-related *Nitrosomonas* (Figure 8). After  
546 organic matter started being fed and cycle configuration was changed (days 147-171), the  
547 abundance of AOB and their population diversity were drastically reduced, with Cluster 6a  
548 members becoming steadily prevalent throughout the rest of Stages II and III. In this sense,  
549 Ma, et al. [32] reported that Cluster 6a phylotypes dominated the nitrifying biomass of an SBR  
550 treating semi-synthetic wastewater bearing similar ranges of concentration of organic matter  
551 and ammonia; in addition, these authors found that Cluster 6a-related populations survived  
552 well to anoxic starvation and were able to fast recover the ammonia oxidation activity after  
553 resuming operation, in line with the observations presented here.



554 **Figure 8.** Heatmap displaying the relative abundances (%) of OTUs classified within the genera  
 555 *Nitrosomonas* and *Nitrosospira*, according to the Illumina sequencing data of the total Bacteria  
 556 communities in the SBR samples retrieved during Stages II and III. Data represent mean (n=2)  
 557 of two independent amplicon samples, SD for the classification levels were less than 1%.

559  
 560 The relative abundance of *Nitrosospira*-related OTUs within the total bacterial community was  
 561 >100-fold reduced in samples of days 231 and 266, in agreement with the trends observed  
 562 when *nxB* copies were quantified by qPCR. The NOB community displayed low diversity since  
 563 only three OTUs related to members of this functional group were identified. Alignment of  
 564 their consensus 16S rRNA sequences against the EMBL database revealed that OTU0157 and  
 565 OTU0324 were close to *Candidatus N. defluvii* (97 % and 99.3 % similarity with accession No.  
 566 DQ059545.1, respectively) while OTU1760 was 99.1 % similar to the sequence of *Candidatus N.*

567 moscoviensis (accession No. AF155153.1). OTU0157 and OTU0324 coexisted in all samples of  
568 Stage II while OTU1760 occurred in very low abundance in the middle phase of Stage II.  
569 Relative abundances of the OTU0157 and OTU0324 abruptly decreased from day 147 onwards,  
570 after the cycle configuration was modified. OTU0324 was the only NOB-related phylotype  
571 detectable in Stage III. According to these results, the diversity of the NOB community was  
572 only slightly modified and not drastically influenced by operational changes, unlike reported by  
573 other authors, who observed NOB population succession at the genus level (from *Nitrospira* to  
574 *Nitrotoga*) in response to FNA [10].

### 575 **3.7. Robustness and feasibility of the *in-situ* FNA inhibitory concentration strategy**

576 In the present study, the nitrification process was started up using a sludge with negligible NOB  
577 activity. Then, stable long-term nitrification process (354 days, 191 treating municipal  
578 wastewater) was achieved by maintaining *in-situ* FNA inhibitory concentrations, from 0.02 to  
579 0.20 mg HNO<sub>2</sub>-N/L, while treating primary settled municipal wastewater at 15 ± 1 °C (Figure 1).  
580 Moreover, no adverse effects associated with the presence of organic matter were observed.  
581 Indeed, an 80 % average organic matter conversion was achieved, limiting the possible growth  
582 of heterotrophic denitrifying bacteria that would compete for nitrite with AMX in the following  
583 anoxic unit.

584 Despite the wastewater composition variability (Table 1), the *in-situ* FNA production-based  
585 strategy was proved to be very robust even when during Stage II the FNA concentration was  
586 below the 0.02 mg HNO<sub>2</sub>-N/L (no NOB activity was observed) or higher than 0.2 mg HNO<sub>2</sub>-N/L  
587 (AOB were not suppressed). Although NOB were present during the entire operational period  
588 (Figure 4) its activity inside the reactor was not observed, confirming the robustness of the *in-*  
589 *situ* FNA strategy. On the contrary, Ma, et al. [10] observed that when the nitrogen  
590 concentration decreased by 28 %, the excess of aeration caused the decrease of NAR from 75

591 to 10 %. In their study, after the increase of influent ammonium concentration, NAR was not  
592 reestablished and the increases of FNA concentration (from 0.25 to 1.00 mg N/L) and sludge  
593 treatment fraction (10 to 30 %) caused an AOB activity reduction while nitrate remained as the  
594 main oxidation product. Jin, et al. [5] achieved long-term stable nitrification operation (260  
595 days) based on the ammonium valley control treating municipal wastewater. Nevertheless,  
596 when a failure in the control system occurred, the DO concentration increased over 2 mg O<sub>2</sub>/L  
597 and nitrate production was observed. In the present strategy, the DO concentration was not  
598 controlled and it only affected the oxidation ratio, while similar nitrate production was not  
599 observed when feeding concentration varied or a failure in the feeding pump or aeration  
600 occurred.

601 Moreover, with the *in-situ* FNA production strategy, no long-term adaptation of NOB to the  
602 suppression factor has been observed (Figure 1), as it has been widely reported when FNA  
603 treatment is applied in an external unit [9]. For example, Ma, et al. [10] noticed a dominant  
604 NOB population shift from *Nitrospira* to *Nitrotoga* genus after the establishment of the  
605 nitrification process by treating the sludge in a FNA treatment unit using 0.75 HNO<sub>2</sub>-N/L and  
606 nitrate build-up was observed. Therefore, it seems that the strategy of NOB activity  
607 suppression by *in-situ* FNA inhibitory concentration is more robust than *ex-situ* treatment.

608 The proposed *in-situ* FNA production-based strategy depends on the N/IC ratio. Pedrouso, et  
609 al. [11] explained that for N/IC ratios between 0.6 to 1.0 g N/g C in incoming wastewater, the  
610 limited alkalinity decreases the pH leading to high FNA concentrations. The feasibility of this  
611 strategy was demonstrated in this study with a N/IC ratio between 0.61 - 0.80 g N/g IC. The  
612 strategy succeeded even when organic matter, traditionally considered as a challenge, was  
613 present. Indeed, *Nitrospira* spp. (the only NOB genus detected) abundance was found  
614 positively correlated to the N/IC ratio of influent wastewater (Figure 7, Table S5). Thus, the

615 application of the *in-situ* FNA inhibitory concentration strategy in those regions characterized  
616 by hard waters ( $N/IC < 0.6 \text{ g N/g IC}$ ) would not be adequate or would require control of pH with  
617 the associated high costs. Nevertheless, more than 50 % of the water in Europe is classified as  
618 soft or slightly hard. Apart from the wastewater hardness (associated with that of freshwater),  
619 the incoming nitrogen and IC concentrations are also influenced by the previous treatment  
620 stages in the WWTP. The most common approaches to remove the organic matter content  
621 from the wastewater are: high rate activated sludge (alkalinity is not significantly affected),  
622 wastewater anaerobic digestion (alkalinity is produced), and/or chemical enhanced pre-  
623 treatment (consumes alkalinity) [53]. Thus, the treatment train must be considered globally to  
624 define the correct operational strategy of the subsequent nitrification unit.

625 To sum up, the proposed strategy enables to maintain stable nitrification process at low  
626 temperature and low nitrogen concentration making possible its application on mainstream  
627 WWTPs and potentially to reach the energy autarky. The advantages of the *in-situ* FNA  
628 production strategy rely on the proven robustness against wastewater composition, and a  
629 complex control system is not required either chemical addition for pH adjustment, among  
630 others.

#### 631 **4. Conclusions**

632 A nitrification process was successfully established and maintained in an SBR by the *in-situ* FNA  
633 accumulation-based strategy (up to  $0.2 \text{ mg HNO}_2/\text{L}$ ) to treat municipal wastewater containing  
634 organic matter (up to  $1.2 \text{ g TOC/N}$ ) at low temperature ( $15 \pm 1 \text{ }^\circ\text{C}$ ). The optimization of the  
635 operational cycle in the SBR allowed coping with the changes in nitrogen and organic matter  
636 concentrations in the municipal wastewater. The results showed that a NAR close to 100 % and  
637 an organic matter removal of 80 % can be achieved in the same unit. Moreover, the long-term  
638 stability (354 days) and robustness of the process were proven despite the influent

639 wastewater composition fluctuations, with N/IC ratios varying from 0.61 to 0.89 g N/g C.  
640 Despite analysis based on microbial molecular markers revealed the occurrence of NOB, their  
641 activity was suppressed due to the high FNA levels achieved by the self-regulation of pH during  
642 the nitrification process. Quantification of bacterial groups by qPCR and analysis of bacterial  
643 diversity by massive parallel sequencing evidenced that both AOB abundance and community  
644 structure were significantly influenced by the concentration of organic matter and the  
645 adjustment of the cycling conditions, while anoxic starvation inflicted a loss of the overall  
646 diversity and promoted specialization of the Bacteria community; however, these changes  
647 were not negatively reflected in the SBR performance, due to functional redundancy within  
648 both the chemoheterotrophic and ammonia oxidizing communities.

#### 649 **Acknowledgements**

650 This work was funded by Pioneer\_STP (PCIN-2015-022 MINECO (AEI)/ID 199 (UE)) project  
651 funded by the WaterWorks2014 Cofunded Call (Water JPI/Horizon 2020) and by the Spanish  
652 Government (AEI) through TREASURE (CTQ2017-83225-C2-1-R) project. Authors from the USC  
653 belong to CRETUS Strategic Partnership (ED431E 2018/01) and to the Galician Competitive  
654 Research Group (GRC ED431C 2017/29). All these programs are co-funded by FEDER (UE).

#### 655 **5. References**

- 656 [1] B. Kartal, L. van Niftrik, J.T. Keltjens, H.J. Op den Camp, M.S. Jetten, Anammox--growth  
657 physiology, cell biology, and metabolism, *Advances in microbial physiology*, 60 (2012) 211-262.  
658 doi: 10.1016/b978-0-12-398264-3.00003-6.
- 659 [2] S. Agrawal, D. Seuntjens, P.D. Cocker, S. Lackner, S.E. Vlaeminck, Success of mainstream  
660 partial nitrification/anammox demands integration of engineering, microbiome and modeling  
661 insights, *Current Opinion in Biotechnology*, 50 (2018) 214-221. doi:  
662 10.1016/j.copbio.2018.01.013.
- 663 [3] A. Pedrouso, I. Aiartza, N. Morales, J.R. Vázquez-Padín, F. Rogalla, J.L. Campos, A.  
664 Mosquera-Corral, A. Val del Rio, Pilot-scale ELAN® process applied to treat primary settled  
665 urban wastewater at low temperature via partial nitrification-anammox processes, *Separation  
666 and Purification Technology*, 200 (2018) 94-101. doi: 10.1016/j.seppur.2018.02.017.
- 667 [4] Q. Yang, Y. Peng, X. Liu, W. Zeng, T. Mino, H. Satoh, Nitrogen Removal via Nitrite from  
668 Municipal Wastewater at Low Temperatures using Real-Time Control to Optimize Nitrifying

669 Communities, *Environmental Science & Technology*, 41 (2007) 8159-8164. doi:  
670 10.1021/es070850f.

671 [5] P. Jin, B. Li, D. Mu, X. Li, Y. Peng, High-efficient nitrogen removal from municipal  
672 wastewater via two-stage nitrification/anammox process: Long-term stability assessment and  
673 mechanism analysis, *Bioresource Technology*, 271 (2019) 150-158. doi:  
674 10.1016/j.biortech.2018.09.097.

675 [6] S. Gu, S. Wang, Q. Yang, P. Yang, Y. Peng, Start up partial nitrification at low temperature  
676 with a real-time control strategy based on blower frequency and pH, *Bioresource Technology*,  
677 112 (2012) 34-41. doi: 10.1016/j.biortech.2011.12.028.

678 [7] Y. Zhou, A. Oehmen, M. Lim, V. Vadivelu, W.J. Ng, The role of nitrite and free nitrous acid  
679 (FNA) in wastewater treatment plants, *Water Research*, 45 (2011) 4672-4682. doi:  
680 10.1016/j.watres.2011.06.025.

681 [8] D. Wang, Q. Wang, A. Laloo, Y. Xu, P.L. Bond, Z. Yuan, Achieving Stable Nitrification for  
682 Mainstream Deammonification by Combining Free Nitrous Acid-Based Sludge Treatment and  
683 Oxygen Limitation, *Scientific Reports*, 6 (2016) 25547. doi: 10.1038/srep25547.

684 [9] H. Duan, L. Ye, X. Lu, Z. Yuan, Overcoming Nitrite Oxidizing Bacteria Adaptation through  
685 Alternating Sludge Treatment with Free Nitrous Acid and Free Ammonia, *Environmental  
686 Science & Technology*, 53 (2019) 1937-1946. doi: 10.1021/acs.est.8b06148.

687 [10] B. Ma, L. Yang, Q. Wang, Z. Yuan, Y. Wang, Y. Peng, Inactivation and adaptation of  
688 ammonia-oxidizing bacteria and nitrite-oxidizing bacteria when exposed to free nitrous acid,  
689 *Bioresource Technology*, 245 (2017) 1266-1270. doi: 10.1016/j.biortech.2017.08.074.

690 [11] A. Pedrouso, Á. Val del Río, N. Morales, J.R. Vázquez-Padín, J.L. Campos, R. Méndez, A.  
691 Mosquera-Corral, Nitrite oxidizing bacteria suppression based on in-situ free nitrous acid  
692 production at mainstream conditions, *Separation and Purification Technology*, 186 (2017) 55-  
693 62. doi: 10.1016/j.seppur.2017.05.043.

694 [12] Y. Jiang, L.S. Poh, C.-P. Lim, W.J. Ng, Impact of free nitrous acid shock and dissolved  
695 oxygen limitation on nitrification maintenance and nitrous oxide emission in a membrane  
696 bioreactor, *Science of The Total Environment*, 660 (2019) 11-17. doi:  
697 10.1016/j.scitotenv.2019.01.024.

698 [13] E.A. Giustinianovich, J.-L. Campos, M.D. Roeckel, A.J. Estrada, A. Mosquera-Corral, Á. Val  
699 del Río, Influence of biomass acclimation on the performance of a partial nitrification-anammox  
700 reactor treating industrial saline effluents, *Chemosphere*, 194 (2018) 131-138. doi:  
701 10.1016/j.chemosphere.2017.11.146.

702 [14] C.E. Bower, T. Holm-Hansen, A Salicylate–Hypochlorite Method for Determining Ammonia  
703 in Seawater, *Canadian Journal of Fisheries and Aquatic Sciences*, 37 (1980) 794-798. doi:  
704 10.1139/f80-106.

705 [15] A. American Public Health Association, A.W.W.A. AWWA, W. Water Pollution Control  
706 Federation, Standard methods for the examination of water and wastewater, 23rd ed., APHA-  
707 AWWA-WPCF, New York, 2017.

708 [16] J. Lopez-Fiuza, B. Buys, A. Mosquera-Corral, F. Omil, R. Mendez, Toxic effects exerted on  
709 methanogenic, nitrifying and denitrifying bacteria by chemicals used in a milk analysis  
710 laboratory, *Enzyme and Microbial Technology*, 31 (2002) 976-985. doi: 10.1016/S0141-  
711 0229(02)00210-7.

712 [17] P. Maza-Marquez, R. Vilchez-Vargas, N. Boon, J. Gonzalez-Lopez, M.V. Martinez-Toledo, B.  
713 Rodelas, The ratio of metabolically active versus total Mycolata populations triggers foaming in  
714 a membrane bioreactor, *Water Res*, 92 (2016) 208-217. doi: 10.1016/j.watres.2015.12.057.

715 [18] S.A. Bustin, V. Benes, J.A. Garson, J. Hellems, J. Huggett, M. Kubista, R. Mueller, T.  
716 Nolan, M.W. Pfaffl, G.L. Shipley, J. Vandesompele, C.T. Wittwer, The MIQE guidelines:  
717 minimum information for publication of quantitative real-time PCR experiments, *Clinical  
718 chemistry*, 55 (2009) 611-622. doi: 10.1373/clinchem.2008.112797.

719 [19] P. Maza-Márquez, R. Vílchez-Vargas, A. González-Martínez, J. González-López, B. Rodelas,  
720 Assessing the abundance of fungal populations in a full-scale membrane bioreactor (MBR)  
721 treating urban wastewater by using quantitative PCR (qPCR), *Journal of Environmental*  
722 *Management*, 223 (2018) 1-8. doi: 10.1016/j.jenvman.2018.05.093.

723 [20] S. Takahashi, J. Tomita, K. Nishioka, T. Hisada, M. Nishijima, Development of a prokaryotic  
724 universal primer for simultaneous analysis of Bacteria and Archaea using next-generation  
725 sequencing, *PloS one*, 9 (2014) e105592-e105592. doi: 10.1371/journal.pone.0105592.

726 [21] P.D. Schloss, S.L. Westcott, T. Ryabin, J.R. Hall, M. Hartmann, E.B. Hollister, R.A.  
727 Lesniewski, B.B. Oakley, D.H. Parks, C.J. Robinson, J.W. Sahl, B. Stres, G.G. Thallinger, D.J. Van  
728 Horn, C.F. Weber, Introducing mothur: Open-Source, Platform-Independent, Community-  
729 Supported Software for Describing and Comparing Microbial Communities, *Applied and*  
730 *environmental microbiology*, 75 (2009) 7537-7541. doi: 10.1128/aem.01541-09.

731 [22] S. Kumar, G. Stecher, M. Li, C. Knyaz, K. Tamura, MEGA X: Molecular Evolutionary Genetics  
732 Analysis across Computing Platforms, *Molecular biology and evolution*, 35 (2018) 1547-1549.  
733 doi: 10.1093/molbev/msy096.

734 [23] M. Henze, W. Gujer, T. Mino, M. van Loosedrecht, *Activated Sludge Models ASM1, ASM2,*  
735 *ASM2d and ASM3*, IWA Publishing, 2006.

736 [24] S. Ge, S. Wang, X. Yang, S. Qiu, B. Li, Y. Peng, Detection of nitrifiers and evaluation of  
737 partial nitrification for wastewater treatment: A review, *Chemosphere*, 140 (2015) 85-98. doi:  
738 10.1016/j.chemosphere.2015.02.004.

739 [25] A. Val del Rio, A. Pichel, N. Fernandez-Gonzalez, A. Pedrouso, A. Fra-Vázquez, N. Morales,  
740 R. Mendez, J.L. Campos, A. Mosquera-Corral, Performance and microbial features of the partial  
741 nitrification-anammox process treating fish canning wastewater with variable  
742 salt concentrations, *Journal of Environmental Management*, 208 (2018) 112-121. doi:  
743 10.1016/j.jenvman.2017.12.007.

744 [26] X. Nan, B. Ma, W. Qian, H. Zhu, X. Li, Q. Zhang, Y. Peng, Achieving nitritation by treating  
745 sludge with free nitrous acid: The effect of starvation, *Bioresource Technology*, 271 (2019) 159-  
746 165. doi: 10.1016/j.biortech.2018.09.113.

747 [27] C. Jiang, S. Xu, R. Wang, S. Zhou, S. Wu, X. Zeng, Z. Bai, G. Zhuang, X. Zhuang,  
748 Comprehensive assessment of free nitrous acid-based technology to establish partial  
749 nitrification, *Environmental Science: Water Research & Technology*, 4 (2018) 2113-2124. doi:  
750 10.1039/C8EW00637G.

751 [28] M. Soliman, A. Eldyasti, Ammonia-Oxidizing Bacteria (AOB): opportunities and  
752 applications—a review, *Reviews in Environmental Science and Bio/Technology*, 17 (2018) 285-  
753 321. doi: 10.1007/s11157-018-9463-4.

754 [29] G. Bitton, *Wastewater Microbiology*, Wiley, 2011.

755 [30] J. Geets, N. Boon, W. Verstraete, Strategies of aerobic ammonia-oxidizing bacteria for  
756 coping with nutrient and oxygen fluctuations, *FEMS Microbiol Ecol*, 58 (2006) 1-13. doi:  
757 10.1111/j.1574-6941.2006.00170.x.

758 [31] A. Elawwad, H. Sandner, U. Kappelmeyer, H. Koeser, Long-term starvation and subsequent  
759 recovery of nitrifiers in aerated submerged fixed-bed biofilm reactors, *Environ Technol*, 34  
760 (2013) 945-959. doi: 10.1080/09593330.2012.722758.

761 [32] F. Ma, A. Li, B. Li, Z. Cui, C. Shi, B. Zhou, Prolonged starvation and subsequent recovery of  
762 nitrification process in a simulated photovoltaic aeration SBR, *Environmental science and*  
763 *pollution research international*, 22 (2015) 10778-10787. doi: 10.1007/s11356-015-4246-8.

764 [33] W. Liu, Q. Yang, B. Ma, J. Li, L. Ma, S. Wang, Y. Peng, Rapid Achievement of Nitritation  
765 Using Aerobic Starvation, *Environmental Science & Technology*, 51 (2017) 4001-4008. doi:  
766 10.1021/acs.est.6b04598.

767 [34] D. Gao, Y. Peng, B. Li, H. Liang, Shortcut nitrification–denitrification by real-time control  
768 strategies, *Bioresource Technology*, 100 (2009) 2298-2300. doi:  
769 10.1016/j.biortech.2008.11.017.

770 [35] A. Nejdat, D. Diaz-Reck, N. Massalha, A. Arbiv, A. Dawas, C. Dosoretz, I. Sabbah,  
771 Abundance and diversity of anammox bacteria in a mainstream municipal wastewater  
772 treatment plant, *Appl Microbiol Biotechnol*, 102 (2018) 6713-6723. doi: 10.1007/s00253-018-  
773 9126-y.

774 [36] S. Wang, Y. Peng, B. Ma, S. Wang, G. Zhu, Anaerobic ammonium oxidation in traditional  
775 municipal wastewater treatment plants with low-strength ammonium loading: Widespread  
776 but overlooked, *Water Research*, 84 (2015) 66-75. doi: 10.1016/j.watres.2015.07.005.

777 [37] Q. Wang, K. Song, X. Hao, J. Wei, M. Pijuan, M.C.M. van Loosdrecht, H. Zhao, Evaluating  
778 death and activity decay of Anammox bacteria during anaerobic and aerobic starvation,  
779 *Chemosphere*, 201 (2018) 25-31. doi: 10.1016/j.chemosphere.2018.02.171.

780 [38] I. Ferrera, O. Sánchez, Insights into microbial diversity in wastewater treatment systems:  
781 How far have we come?, *Biotechnology Advances*, 34 (2016) 790-802. doi:  
782 10.1016/j.biotechadv.2016.04.003.

783 [39] Y. Xia, X. Wen, B. Zhang, Y. Yang, Diversity and assembly patterns of activated sludge  
784 microbial communities: A review, *Biotechnol Adv*, 36 (2018) 1038-1047. doi:  
785 10.1016/j.biotechadv.2018.03.005.

786 [40] D. Shu, H. Yue, Y. He, G. Wei, Divergent assemblage patterns of abundant and rare  
787 microbial sub-communities in response to inorganic carbon stresses in a simultaneous  
788 anammox and denitrification (SAD) system, *Bioresource Technology*, 257 (2018) 249-259.  
789 <https://doi.org/10.1016/j.biortech.2018.02.111>.

790 [41] A. Cydzik-Kwiatkowska, M. Zielińska, Bacterial communities in full-scale wastewater  
791 treatment systems, *World Journal of Microbiology and Biotechnology*, 32 (2016) 66. doi:  
792 10.1007/s11274-016-2012-9.

793 [42] B. Zhang, X. Xu, L. Zhu, Structure and function of the microbial consortia of activated  
794 sludge in typical municipal wastewater treatment plants in winter, *Scientific Reports*, 7 (2017)  
795 17930. doi: 10.1038/s41598-017-17743-x.

796 [43] J.P. Marais, J.J. Therion, R.I. Mackie, A. Kistner, C. Dennison, Effect of nitrate and its  
797 reduction products on the growth and activity of the rumen microbial population, *British*  
798 *Journal of Nutrition*, 59 (1988) 301-313. doi: 10.1079/bjn19880037.

799 [44] H. Duan, S. Gao, X. Li, N.H. Ab Hamid, G. Jiang, M. Zheng, X. Bai, P.L. Bond, X. Lu, M.M.  
800 Chislett, S. Hu, L. Ye, Z. Yuan, Improving wastewater management using free nitrous acid  
801 (FNA), *Water Research*, 171 (2020) 115382. doi: 10.1016/j.watres.2019.115382.

802 [45] B. Wang, Z. Wang, S. Wang, X. Qiao, X. Gong, Q. Gong, X. Liu, Y. Peng, Recovering partial  
803 nitritation in a PN/A system during mainstream wastewater treatment by reviving AOB activity  
804 after thoroughly inhibiting AOB and NOB with free nitrous acid, *Environment International*,  
805 139 (2020) 105684. doi: 10.1016/j.envint.2020.105684.

806 [46] Y. Wang, J. Zhao, D. Wang, Y. Liu, Q. Wang, B.-J. Ni, F. Chen, Q. Yang, X. Li, G. Zeng, Z.  
807 Yuan, Free nitrous acid promotes hydrogen production from dark fermentation of waste  
808 activated sludge, *Water Research*, 145 (2018) 113-124. doi: 10.1016/j.watres.2018.08.011.

809 [47] A.E. Laloo, J. Wei, D. Wang, S. Narayanasamy, I. Vanwonterghem, D. Waite, J. Steen, A.  
810 Kaysen, A. Heintz-Buschart, Q. Wang, B. Schulz, A. Nouwens, P. Wilmes, P. Hugenholtz, Z. Yuan,  
811 P.L. Bond, Mechanisms of Persistence of the Ammonia-Oxidizing Bacteria *Nitrosomonas* to the  
812 Biocide Free Nitrous Acid, *Environmental Science & Technology*, 52 (2018) 5386-5397. doi:  
813 10.1021/acs.est.7b04273.

814 [48] B. Gómez-Villalba, C. Calvo, R. Vilchez, J. González-López, B. Rodelas, TGGE analysis of the  
815 diversity of ammonia-oxidizing and denitrifying bacteria in submerged filter biofilms for the

816 treatment of urban wastewater, *Applied Microbiology and Biotechnology*, 72 (2006) 393-400.  
817 doi: 10.1007/s00253-005-0272-7.

818 [49] S. Siripong, B.E. Rittmann, Diversity study of nitrifying bacteria in full-scale municipal  
819 wastewater treatment plants, *Water Research*, 41 (2007) 1110-1120. doi:  
820 10.1016/j.watres.2006.11.050.

821 [50] H. Daims, M. Wagner, The microbiology of nitrogen removal, in: N.P.E. Seviour RJ (Ed.)  
822 *Microbial Ecology of Activated Sludge*, IWA Publishing, 2010, pp. 259-280.

823 [51] C.J. Sedlacek, B. McGowan, Y. Suwa, L. Sayavedra-Soto, H.J. Laanbroek, L.Y. Stein, J.M.  
824 Norton, M.G. Klotz, A. Bollmann, A Physiological and Genomic Comparison of Nitrosomonas  
825 Cluster 6a and 7 Ammonia-Oxidizing Bacteria, 78 (2019) 985-994. doi: 10.1007/s00248-019-  
826 01378-8.

827 [52] A. Bollmann, M.J. Bar-Gilissen, H.J. Laanbroek, Growth at low ammonium concentrations  
828 and starvation response as potential factors involved in niche differentiation among ammonia-  
829 oxidizing bacteria, *Applied and environmental microbiology*, 68 (2002) 4751-4757. doi:  
830 10.1128/aem.68.10.4751-4757.2002.

831 [53] H. Guven, R.K. Dereli, H. Ozgun, M.E. Ersahin, I. Ozturk, Towards sustainable and energy  
832 efficient municipal wastewater treatment by up-concentration of organics, *Progress in Energy  
833 and Combustion Science*, 70 (2019) 145-168. doi: 10.1016/j.pecs.2018.10.002.

834